

## REPORT No. 675

# EFFECTS OF ELEVATOR NOSE SHAPE, GAP, BALANCE, AND TABS ON THE AERODYNAMIC CHARACTERISTICS OF A HORIZONTAL TAIL SURFACE

By HARRY J. GOETT and J. P. REEDER

### SUMMARY

Results are presented showing the effects of gap, elevator nose shape, balance, cut-out, and tabs on the aerodynamic characteristics of a horizontal tail surface tested in the N. A. C. A. full-scale tunnel.

The presence of a gap caused an 18 percent reduction in the variation of normal force with elevator deflection but the size of the gap (between  $0.005\bar{c}$  and  $0.010\bar{c}$ ) was an unimportant factor. At small elevator deflections, the effectiveness of aerodynamic balance of the elevator in reducing hinge moments was much lower with the tapered nose than with the blunt nose. The tapered nose, however, maintained its effectiveness to much greater deflections and gave a greater maximum normal-force increment than did the blunt nose. With the blunt nose, the hinge moments were reduced 30 and 40 percent with 10- and 20-percent balances, respectively. This reduction is fairly uniform up to the stall of the elevator. The decrease in normal force and hinge moment caused by a cut-out was proportional to the area removed. The variation in tab effectiveness with a change in tab span was found to be approximately proportional to the area-moment of the tab about the elevator hinge line. A comparison of the various experimental aerodynamic characteristics with those computed from Glauert's thin-airfoil theory for hinged flaps is also given.

### INTRODUCTION

The tail-surface investigation being carried on in the N. A. C. A. full-scale wind tunnel includes the determination of isolated tail-surface characteristics and the variation in these characteristics caused by wing, fuselage, and slipstream interference. The subject report deals with certain factors influencing the characteristics of the isolated tail surface.

Examination of existing data shows a lack of information in regard to the effect of elevator nose shape and gap upon tail-surface characteristics, particularly with reference to aerodynamic balance of the elevator. Data are also lacking concerning the effects of elevator cut-out and of trailing-edge tabs on large-chord flaps. The importance of some of these variables is indicated in references 1 and 2. The tests reported herein were therefore carried out to determine the effects of these

factors on a tail surface of representative design. In the analysis, the differences between the experimental results and those obtained from the thin-airfoil theory have been indicated so that the conclusions may be readily generalized.

### SYMBOLS

The symbols used in the report are defined as follows:

- $A$ , aspect ratio.
- $R$ , Reynolds Number.
- $C_N$ , normal-force coefficient ( $C_L \cos \alpha + C_D \sin \alpha$ ).
- $C_C$ , chord-force coefficient ( $C_D \cos \alpha - C_L \sin \alpha$ ).
- $H_e$ , elevator hinge moment.
- $C_{h_e}$ , elevator hinge-moment coefficient  $\frac{H_e}{q c_e b_e}$ .
- $\Delta C_{h_e}$ , change in  $C_{h_e}$  with  $\delta_e$ .
- $\alpha$ , angle of attack of the tail, deg.
- $\delta_e$ , elevator angle (downward deflection positive).
- $\delta_t$ , tab angle (downward deflection positive).
- $S$ , area.
- $b$ , span.
- $c$ , chord.
- $\bar{c}$ , average chord.
- $c_e^2$ , mean square of elevator chords.
- $a_0$ , slope of section lift or normal-force curve (per deg.).
- $a_1$ , slope of lift or normal-force curve, elevator fixed (per deg.).

Subscripts:

- $e$ , elevator.
- $b$ , balance.
- $t$ , tab.

Symbols with no subscripts refer to the entire horizontal tail surface.

### APPARATUS

The tests were conducted in the full-scale wind tunnel described in reference 3. The tail surface is shown mounted in the tunnel jet in figure 1.

The dimensions of the tail surface are given in figure 2. The taper ratio was 2:1 and the locus of the 0.55 $\bar{c}$  stations (the hinge line) was perpendicular to the line of symmetry. The  $S_e/S$  ratio was 0.41 and the aspect ratio was 4.7. The cut-out area was equal to 3 percent of the tail area.

Removable elevator-nose and stabilizer-tail blocks (see fig. 3) were provided so that the elevator balance, the nose shape, and the gap could be varied. Provision was made for minimum, 10-percent, and 20-percent



FIGURE 1.—Tail surface mounted in the full-scale tunnel.

balances with the balance distributed along the span of the elevator in proportion to the local chord. With the minimum-balance nose, 4 percent of the elevator area projected forward of the hinge line but, since this overhang was less than the section thickness at the hinge

Provision was made on all the arrangements for  $\frac{1}{4}$ -inch and  $\frac{1}{2}$ -inch gaps, equal to 0.005 $\bar{c}$  and 0.010 $\bar{c}$ . Zero gap was obtained for the minimum balance by sealing the gap.

The trailing-edge tab, equal to 18 percent of the elevator area, was divided into inboard, middle, and outboard sections of approximately equal areas that could be individually deflected.

The device for the measurement of the elevator hinge moment was housed in the center section of the tail and consisted of a calibrated torsion rod to which the hinge moment was transmitted. The deflection of this rod caused the rotation of a self-synchronous motor in the tail, which in turn controlled a similar motor in the scale house where the deflection was measured.

**TESTS**

Preliminary tests were made to determine the tare, the blocking, and the tunnel corrections according to the procedure outlined in reference 4.

Lift, drag, and hinge moments were measured on the following tail arrangements for elevator deflections from 0° to 30° and for angles of attack from -12° to 20°.

- (1) Minimum balance, zero gap (no hinge moments measured).
- (2) Minimum balance, 0.005 $\bar{c}$  and 0.010 $\bar{c}$  gaps.
- (3) Minimum balance, 0.005 $\bar{c}$  gap, cut-out covered.

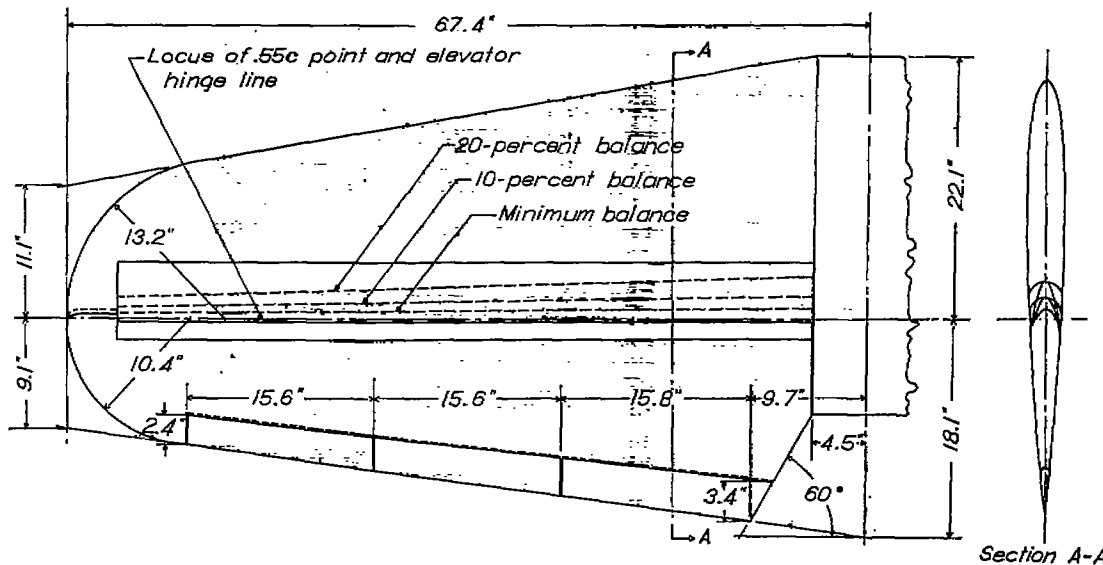


FIGURE 2.—Horizontal tail surface. Total area, 27 sq. ft.; stabilizer area, 15.9 sq. ft.; elevator area, 11.1 sq. ft.; taper ratio, 2:1; aspect ratio, 4.7; airfoil section, N. A. C. A. 0009.

line, this arrangement was used for comparison with zero-balance results computed from thin-airfoil theory. The blunt and the tapered nose shapes are shown in figure 3. The blunt nose was formed by making the leading-edge radius equal to one-half the section thickness. Only one nose shape was provided for the minimum balance; it has been used for comparison with both the blunt and the tapered noses of the 10- and the 20-percent balances.

- (4) Minimum balance, 0.005 $\bar{c}$  gap, tab deflections from 0° to -30°, with:
  - (a) Full-span tabs.
  - (b) Inboard and middle tabs.
  - (c) Inboard tabs.
  - (d) Middle tabs.
  - (e) Outboard tabs.
- (5) 10-percent balance, tapered nose, 0.005 $\bar{c}$  and 0.010 $\bar{c}$  gaps.

(6) 10-percent balance, blunt nose, 0.005 $\bar{c}$  and 0.010 $\bar{c}$  gaps.

(7) 20-percent balance, tapered nose, 0.005 $\bar{c}$  and 0.010 $\bar{c}$  gaps.

(8) 20-percent balance, blunt nose, 0.005 $\bar{c}$  and 0.010 $\bar{c}$  gaps.

All the foregoing tests were conducted at a tunnel air speed of 65 miles per hour corresponding to a Reynolds Number of 1,460,000 based on the average chord. Further tests between speeds of 25 and 80 miles per hour were made to determine the scale effect on elevator hinge moments.

**RESULTS AND DISCUSSION**  
**NORMAL-FORCE CHARACTERISTICS**

The variation of normal-force coefficient and chord-force coefficient with angle of attack for various arrangements of elevator balance, nose shape, and gap and for elevator deflections from 0° to 30° is given in figures 4 to 9. The  $C_G$  curves for the 0.010 $\bar{c}$  gap arrangements are omitted because they are the same as those for the 0.005 $\bar{c}$  gap except in the region of the stall.

The slope of the normal-force coefficient,  $dC_N/d\alpha$ , for an N. A. C. A. 0009 airfoil of 4.7 aspect ratio and 2:1 taper, as computed from the aspect-ratio correction formula (see the appendix), is 0.069. This value is to be compared with the experimental slope of 0.063 obtained for the zero-gap condition (fig. 4), which was reduced to 0.060 when a gap was introduced (fig. 5). It will be noted that, for elevator deflections up to 10°, the deflections, the nose shape, and the gap size had a negligible effect on the slope, causing not more than a  $\pm 0.002$  variation from the average value of 0.060; at a  $\delta_e$  of 20°, the average slope decreased to about 0.056. Tests with the elevator cut-out covered showed no change in slope when the coefficients were based on the increased area.

The effect of the gap appears on the  $C_N$  curves mainly as a shift in the angle of zero lift for elevator deflections other than zero. This shift causes a decrease in the  $dC_N/d\delta_e$  slope for the arrangements with gap, which will be noted in figure 10 (a). The zero-gap arrangement has a slope of 0.043 (up to  $\delta_e$  of 15°), which is decreased to approximately 0.032 when a gap is introduced. These slopes are, respectively, 93 percent and 75 percent of the corresponding slopes computed from thin-airfoil theory. (See equation (1), appendix.) The difference in slope between the 0.005 $\bar{c}$  and the

0.010 $\bar{c}$  arrangements is small at angles below the stall. For some nose shapes, the larger gap causes an earlier stall. (See  $\delta_e=20^\circ$  and  $30^\circ$ , fig. 8.)

The addition of aerodynamic balance increases the  $dC_N/d\delta_e$  slope (figs. 10 (b) and (c)). The tapered nose gives a slightly lower slope at small elevator deflections than do the blunt noses, probably because of the more marked shielding effect of the stabilizer. The tapered

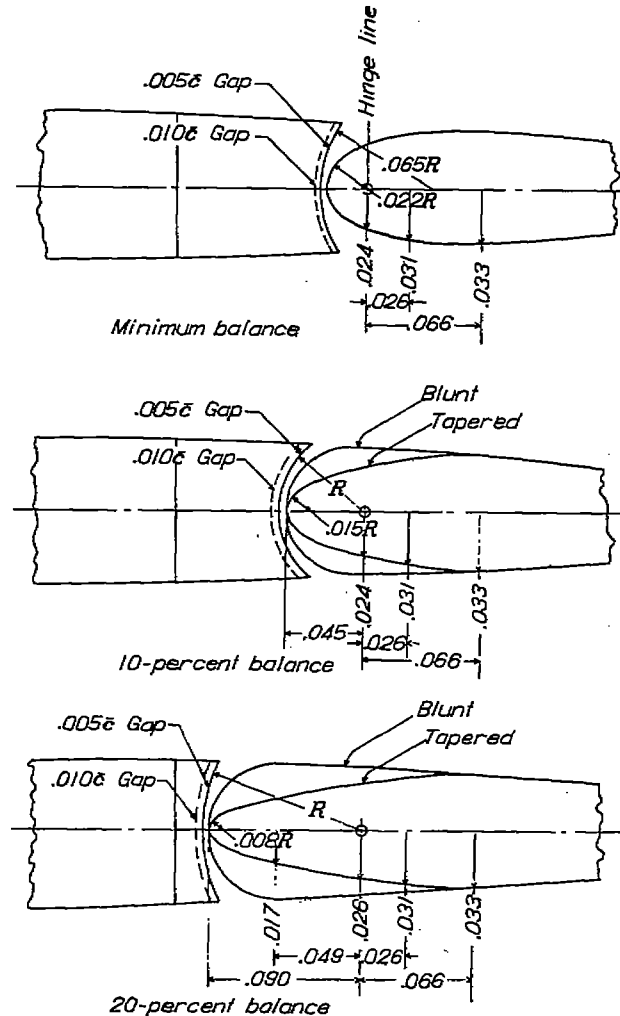


FIGURE 3.—Elevator-nose and stabilizer-tail blocks of the horizontal-tail surface. Nose ordinates given in fractions of local chord.

nose, however, permits the maintenance of elevator effectiveness to much larger deflections and gives a greater maximum increment of normal-force coefficient. For instance, the 20-percent-balance blunt nose gives a maximum increment of only 0.75, as compared with a value of 1.05 obtainable with the tapered nose of equal balance.

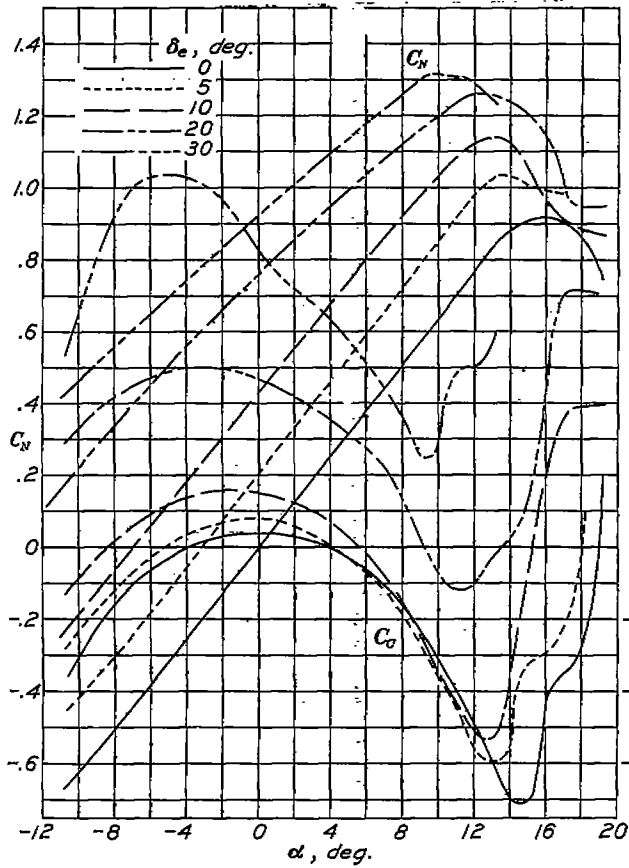


FIGURE 4.—Variation of  $C_N$  and  $C_D$  with  $\alpha$  at various elevator deflections for minimum balance, zero gap.

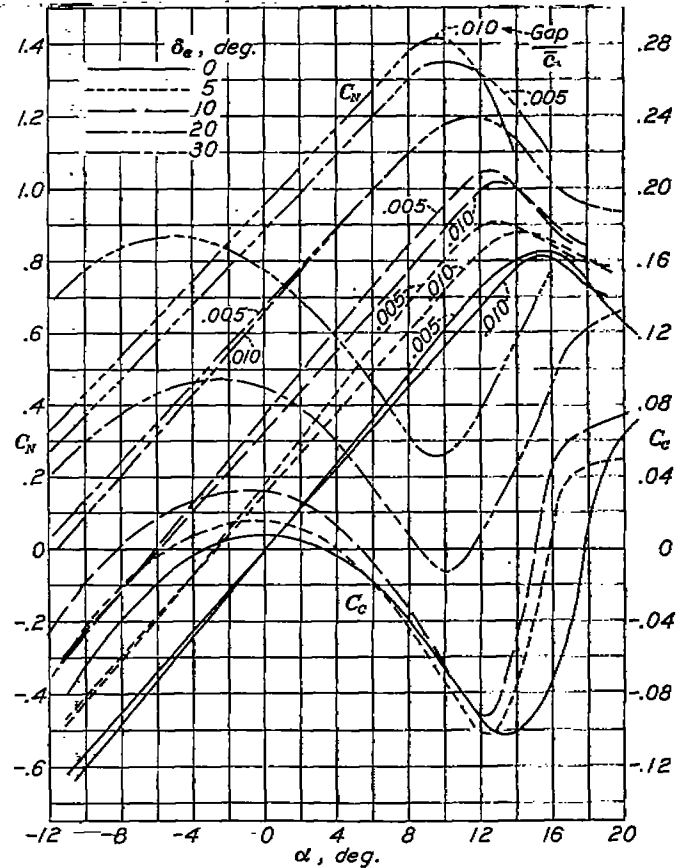


FIGURE 6.—Variation of  $C_N$  and  $C_D$  with  $\alpha$  at various elevator deflections for 10-percent balance, tapered nose, 0.005c and 0.010c gap.

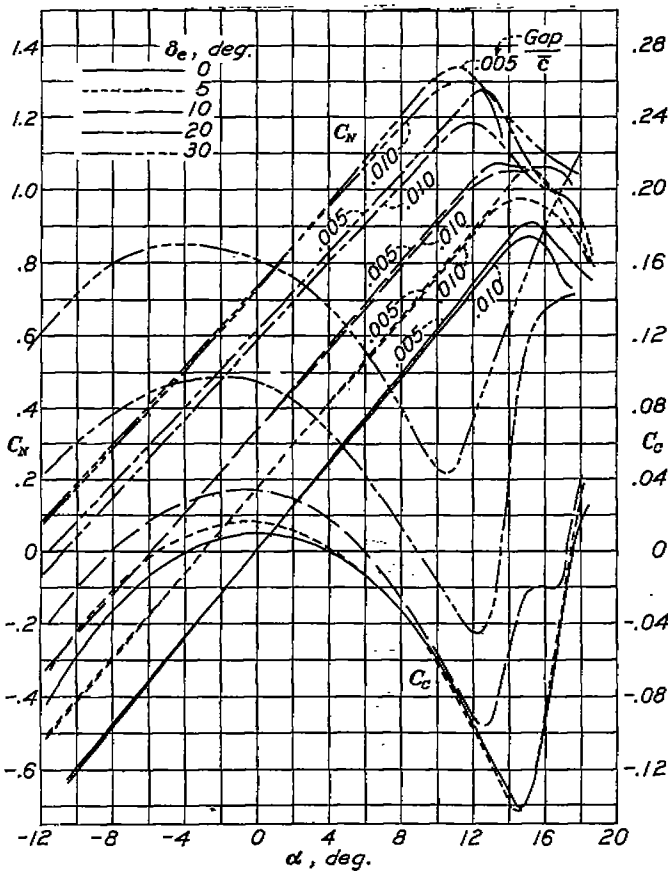


FIGURE 5.—Variation of  $C_N$  and  $C_D$  with  $\alpha$  at various elevator deflections for minimum balance, 0.005c and 0.010c gap.

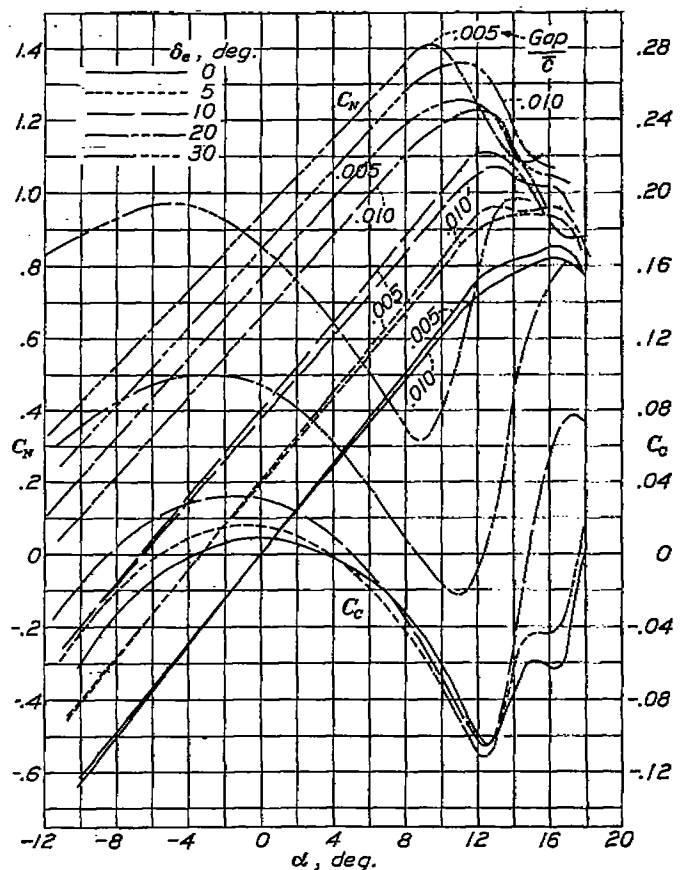


FIGURE 7.—Variation of  $C_N$  and  $C_D$  with  $\alpha$  at various elevator deflections for 10-percent balance, blunt nose, 0.005c and 0.010c gap.



EFFECTS OF ELEVATOR AND TABS ON A HORIZONTAL TAIL SURFACE

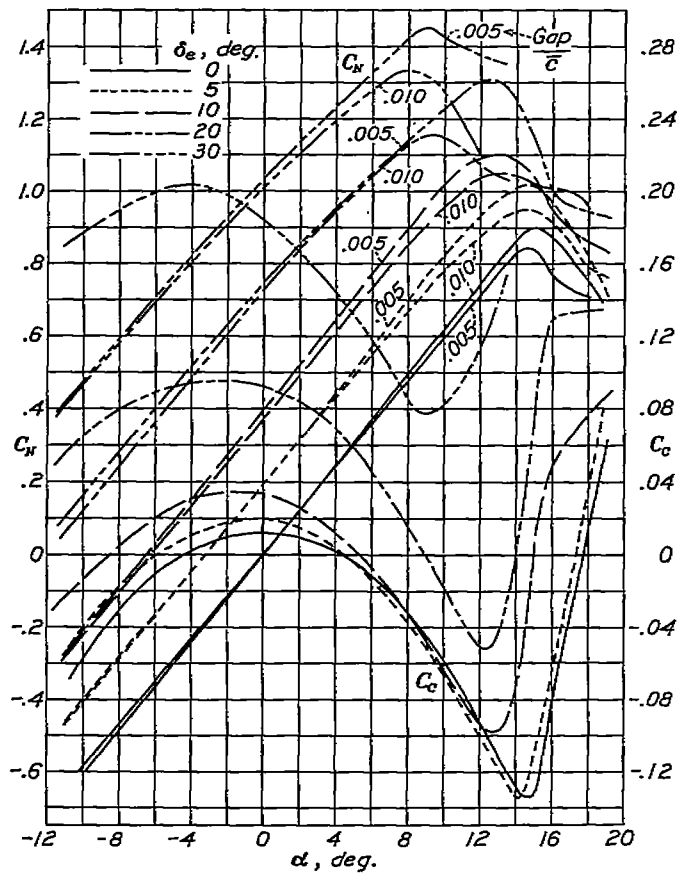


FIGURE 8.—Variation of  $C_x$  and  $C_c$  with  $\alpha$  at various elevator deflections for 20-percent balance, tapered nose, 0.005 and 0.010 gap.

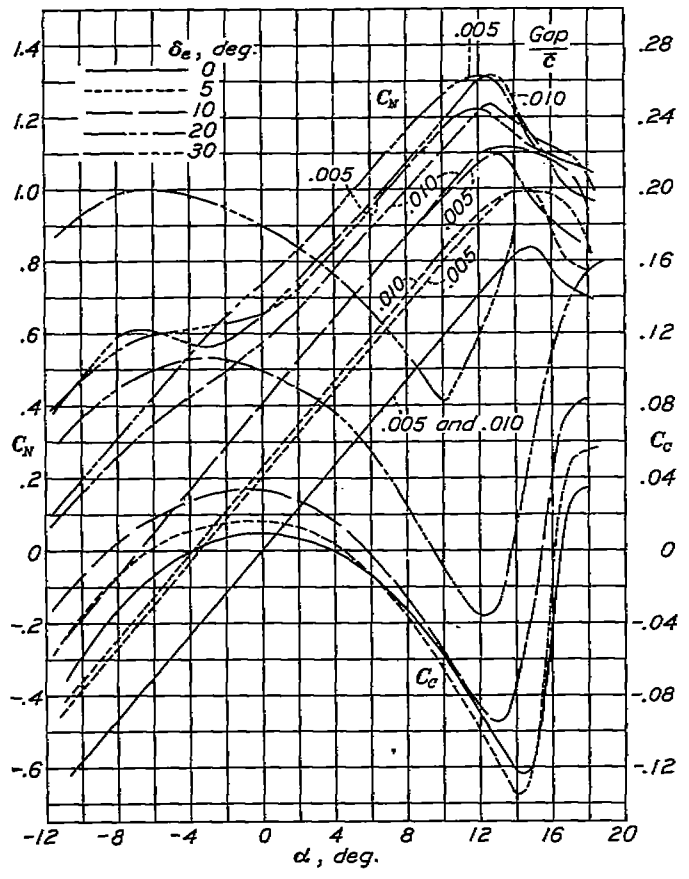


FIGURE 9.—Variation of  $C_x$  and  $C_c$  with  $\alpha$  at various elevator deflections for 20-percent balance, blunt nose, 0.005 and 0.010 gap.

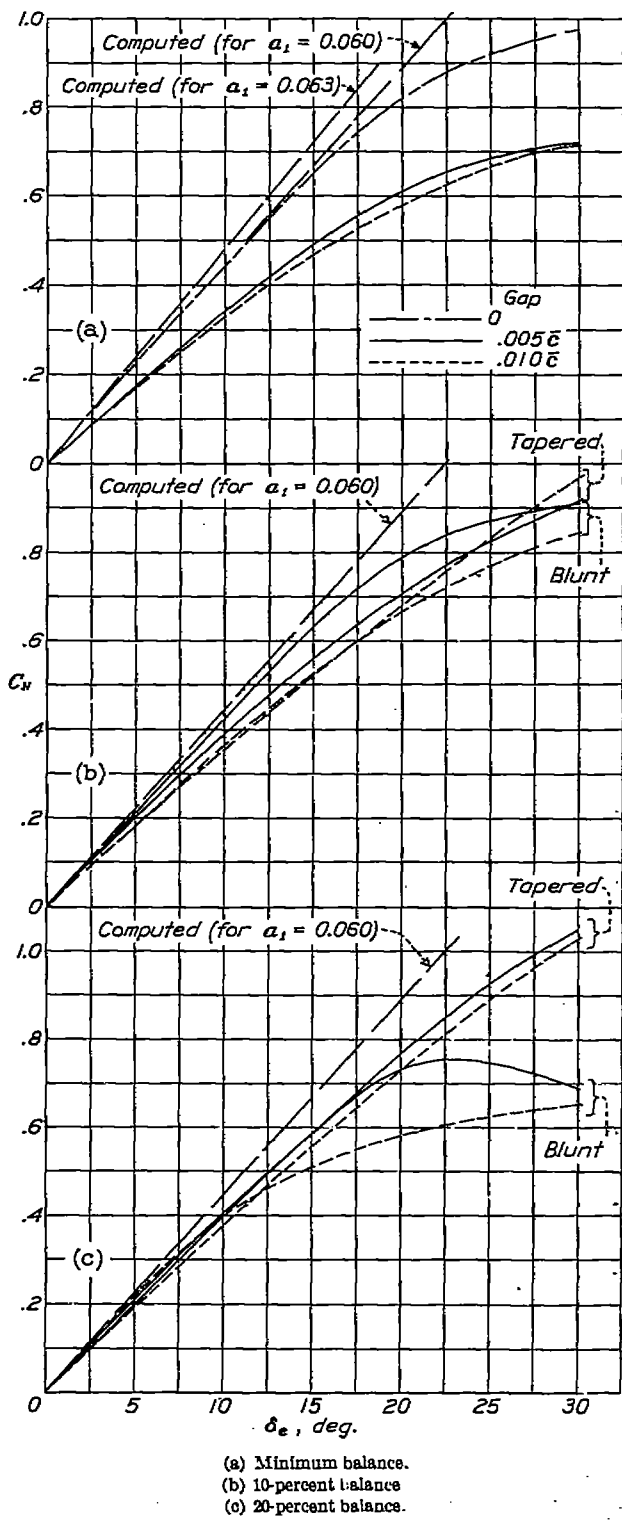


FIGURE 10.—Effect of gap and nose shape on variation of  $C_x$  with  $\delta_e$ .  $\alpha = 0^\circ$

The results shown in figure 10 are for an angle of attack of zero, but they are characteristic of the results obtained within an angle-of-attack range of  $\pm 8^\circ$ .

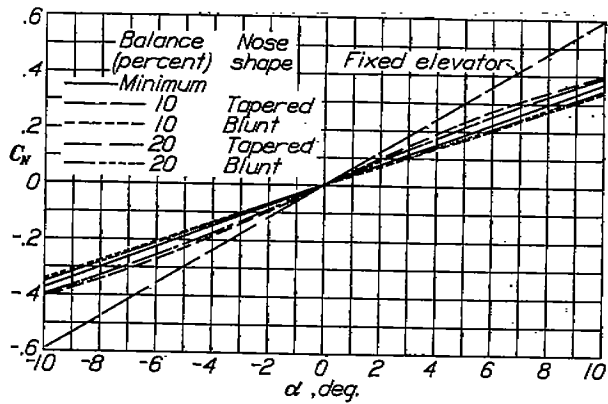
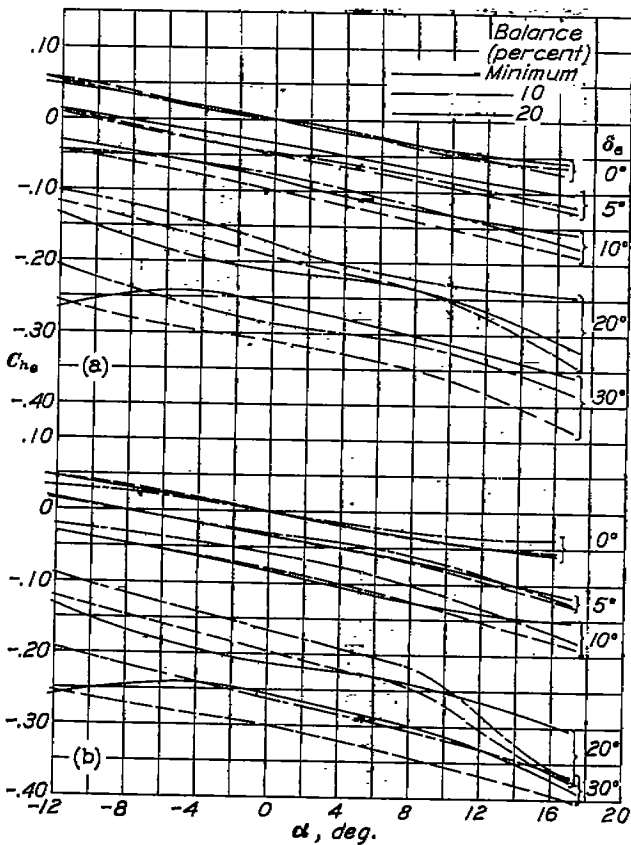


FIGURE 11.—Variation of  $C_N$  with  $\alpha$ . Elevator free; 0.005c gap.



(a) Tapered nose.  
(b) Blunt nose.

FIGURE 12.—Variation of  $C_h$  with  $\alpha$ .

The elevator-free lift-curve slopes for all the tail arrangements with the 0.005c gap are shown in figure 11. The experimental slope for the minimum balance is 0.037; the slope computed from thin-airfoil theory is

0.035. (See equation (2) in appendix.) An investigation of a number of other unbalanced tails, for which data are given in reference 2, shows that this close correspondence between the experimental and the

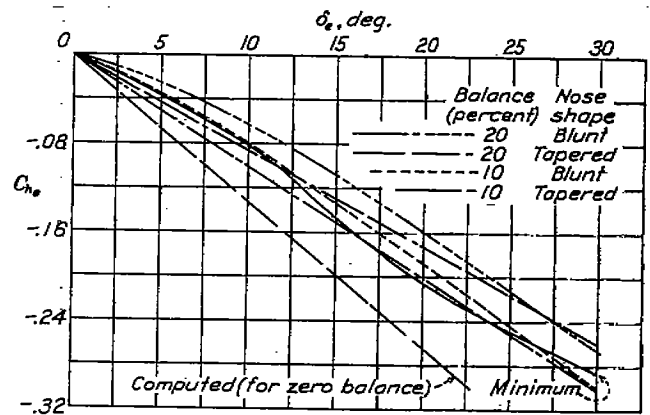
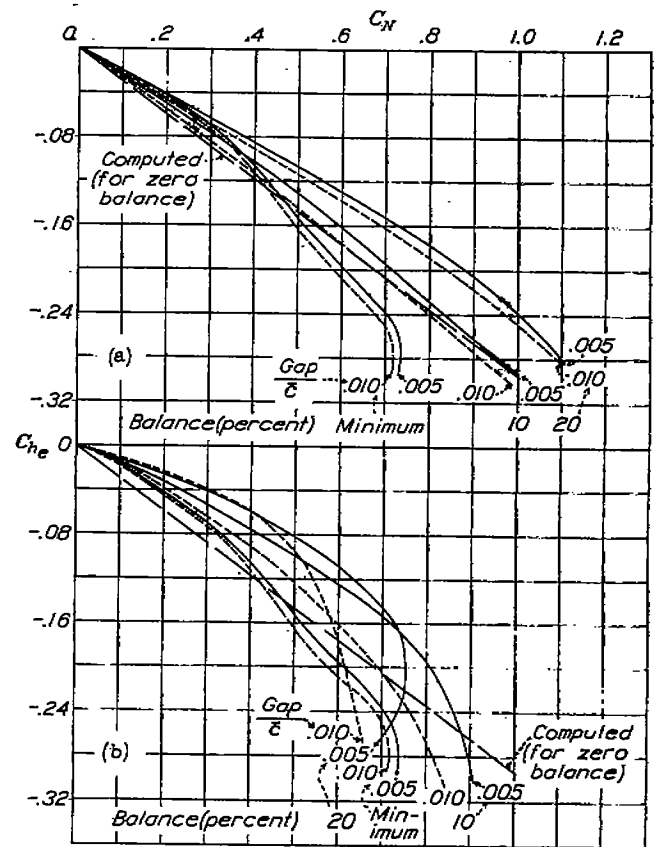


FIGURE 13.—Variation of  $C_h$  with  $\delta_e$ .  $\alpha = 0^\circ$ .



(a) Tapered nose.  
(b) Blunt nose.

FIGURE 14.—Variation of  $C_h$  with  $C_N$ .  $\alpha = 0^\circ$ .

computed slopes is not general. Experimental slopes computed from the results in reference 2 varied from 15 percent to 40 percent in excess of the computed slope.

HINGE-MOMENT CHARACTERISTICS

The variation of hinge-moment coefficient with angle of attack for the various tail arrangements is shown in figure 12. These curves are applicable to both the 0.005c and the 0.010c gap arrangements because the size of these gaps caused negligible variations. The  $dC_{h_e}/d\alpha$  slope computed from thin-airfoil theory is

from  $\pm 8^\circ$ . It will be noted that  $dC_{h_e}/d\delta_e$  varies from 0.55 to 0.75 of the value computed from thin-airfoil theory for an unbalanced elevator. The effect of the cut-out on this slope is proportional to the area removed; the scale effect between speeds of 25 and 80 miles per hour (Reynolds Number equal to 560,000 to

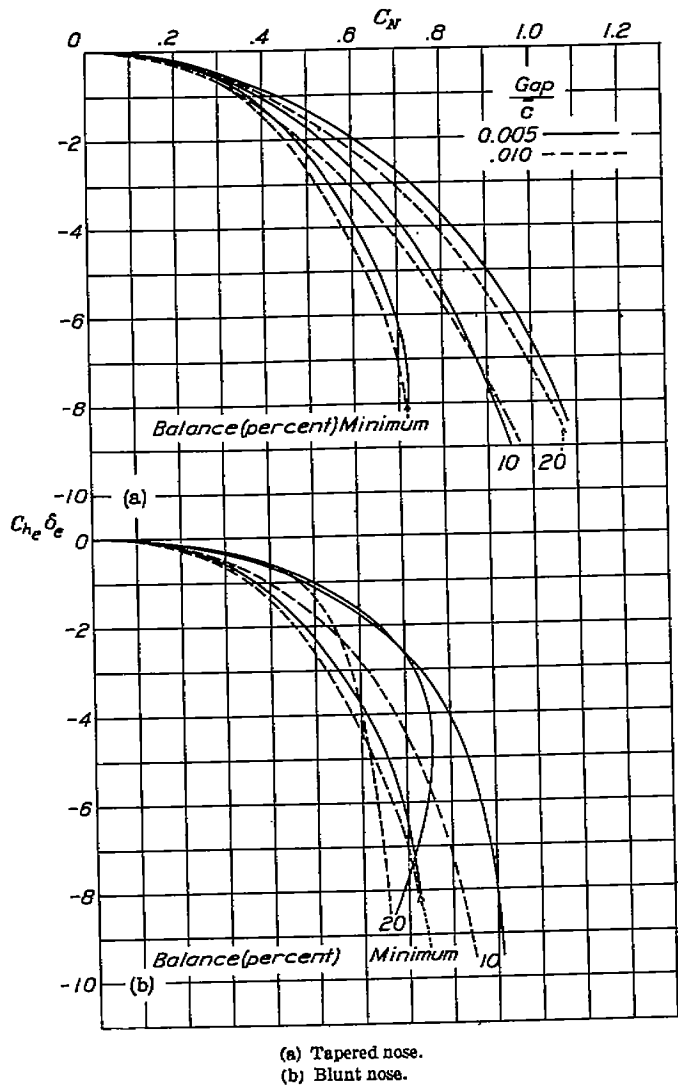


FIGURE 15.—Variation of stick-force criterion  $C_{h_e} \delta_e$  with  $C_N$  for various tab arrangements.  $\alpha = 0^\circ$ .

-0.0073, which compares with an average experimental value of -0.0045. There appears to be no systematic variation of slope with nose shape, balance, or elevator deflection, these factors causing a spread of no more than  $\pm 0.0005$  from the average value.

A cross plot of elevator hinge-moment coefficient against elevator deflection is given in figure 13 for each of the balance and nose-shape arrangements. These curves are for an angle of attack of  $0^\circ$  but are characteristic of the values obtained over a range of angles

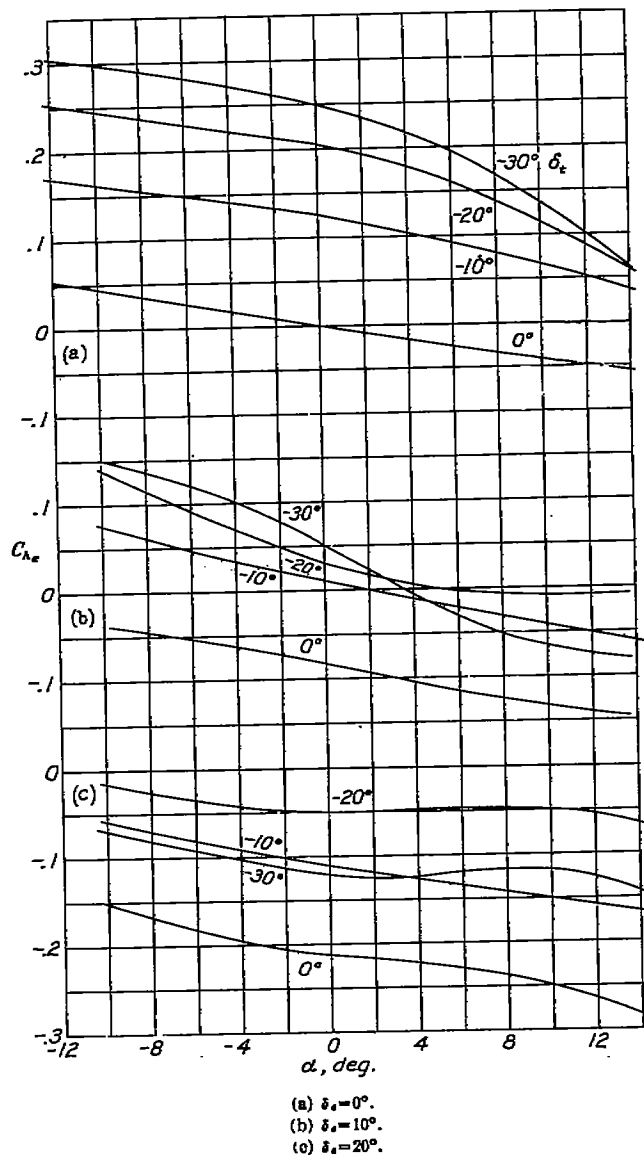


FIGURE 16.—Variation of  $C_{h_e}$  with  $\alpha$  for various deflections of the full-span tab.

1,800,000 based on the average chord) was found to be negligible.

A criterion of balance effectiveness is the reduction produced in  $C_{h_e}$  for a given  $C_N$ . Figure 14 shows this characteristic. A uniform reduction in  $C_{h_e}$  up to the point at which the elevator stalls is obtained with the blunt-nose balances; the balancing effect of the tapered noses, however, varies markedly with elevator deflection but remains effective to much higher values of  $C_N$

than for the blunt noses. Table I summarizes the balancing effect of the various balances and nose shapes. The relatively close agreement of the experimental

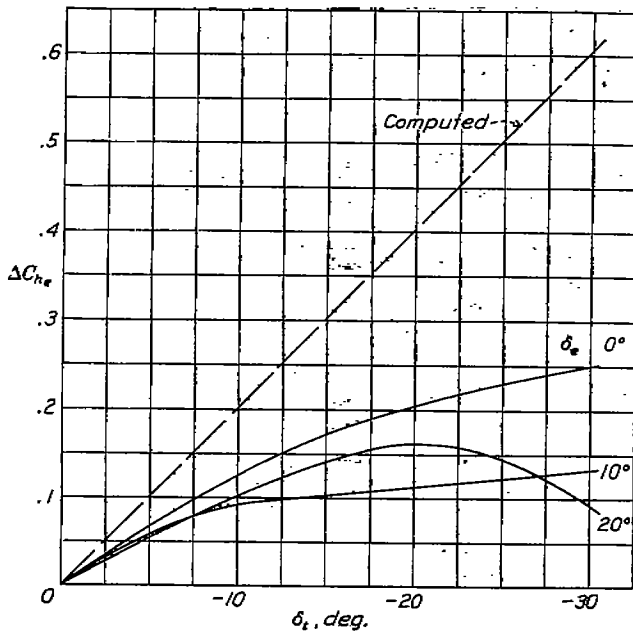


FIGURE 17.—Variation of  $\Delta C_{h_e}$  with  $\delta_e$  for full-span tab.  $\alpha=0^\circ$ .

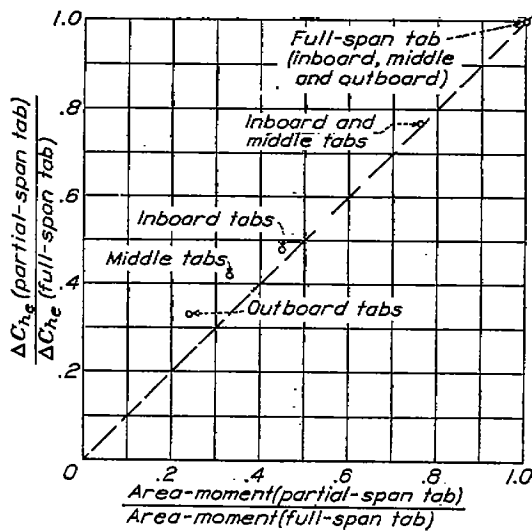
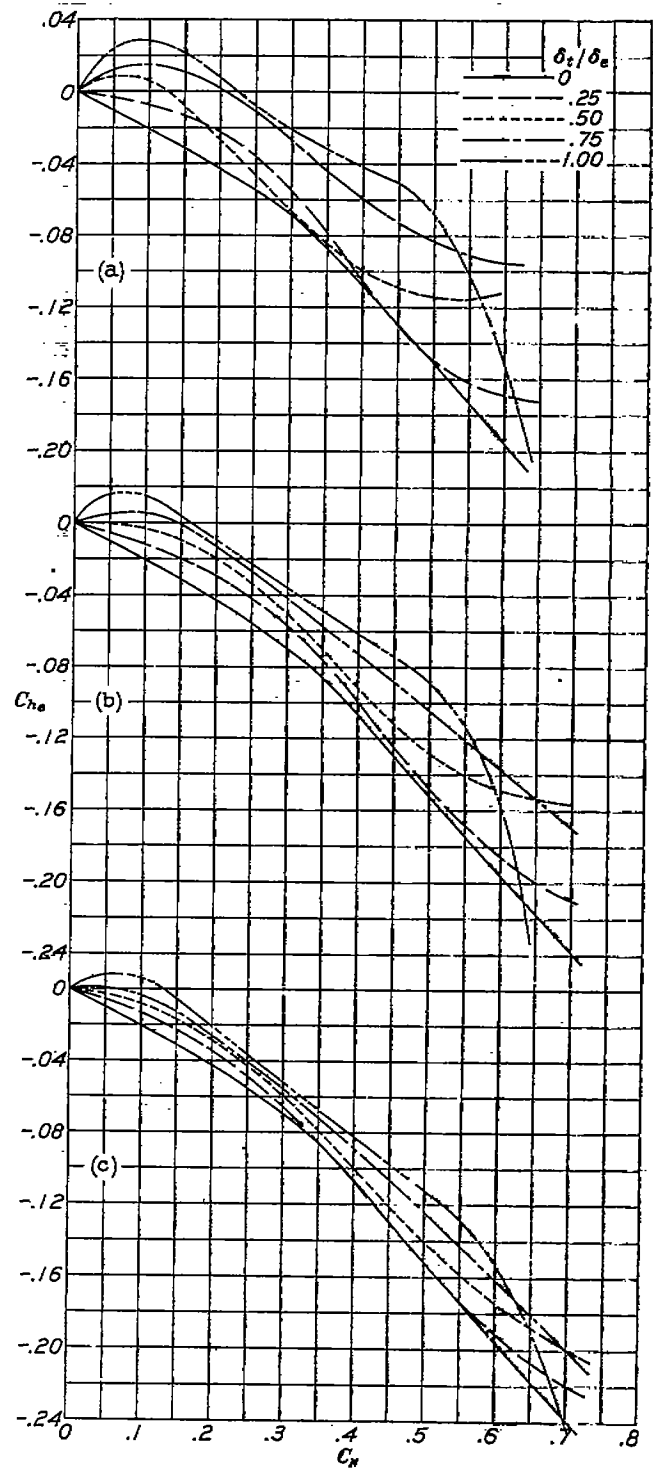


FIGURE 18.—Variation of tab effectiveness with tab span.

$dC_N/dC_{h_e}$  slope compared with that computed by thin-airfoil theory is due to the fact that a decrease in  $dC_N/d\delta_e$  caused by the gap is compensated by a corresponding decrease in  $dC_{h_e}/d\delta_e$ .



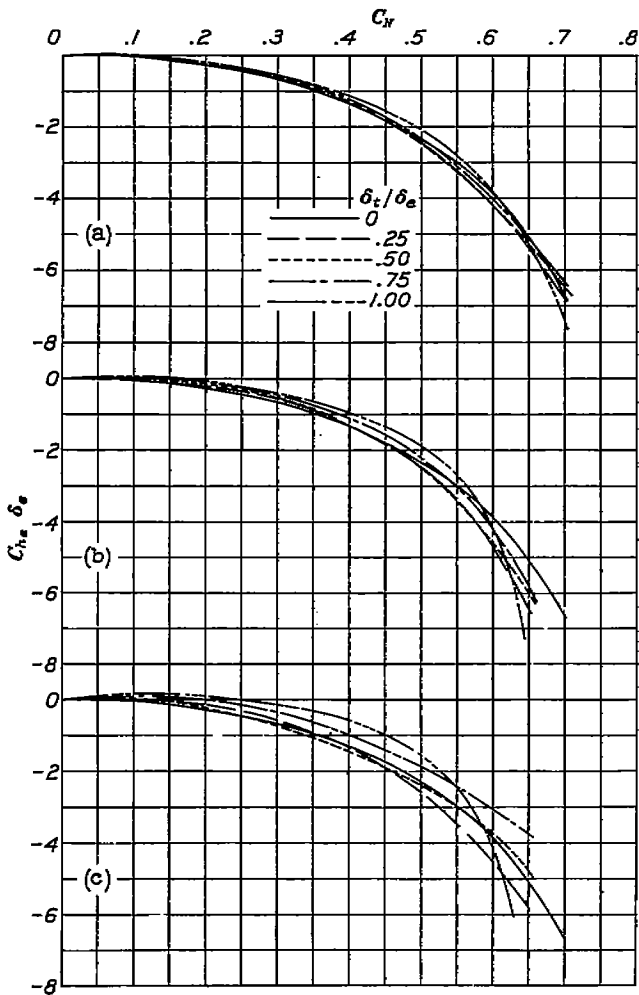
(a) Full-span tab.  
 (b) Inboard and middle tabs.  
 (c) Inboard tab.

FIGURE 19.—Variation of  $C_{h_e}$  with  $C_N$  for various tab span and  $\delta_e/\delta_e$  ratios.  $\alpha=0^\circ$ .



TABLE I  
 REDUCTION IN  $C_{h_e}$  PRODUCED BY VARIOUS BALANCE  
 AND NOSE-SHAPE ARRANGEMENTS; 0.0057 GAP

Balance (percent)	Nose shape	Percentage reduction in $C_{h_e}$ (compared with minimum balance) for a given $C_N$
10	Blunt	30
	Tapered	0-20
20	Blunt	40
	Tapered	0-40



(a) Inboard tab.  
 (b) Inboard and middle tabs.  
 (c) Full-span tabs.

FIGURE 20.—Variation of stick-force criterion,  $C_{h_e} \delta_e$ , with  $C_N$  for various tab arrangements.  $\alpha=0^\circ$ .

Another criterion of balance effectiveness is the variation of  $C_{h_e} \delta_e$  with  $C_N$ . This criterion takes into account the possible reduction in  $C_N$  for a given elevator deflection that may be caused by the balancing device (necessitating a change in the mechanical advantage of the control system). The development of this criterion

is given in detail in reference 5. Figure 15 shows a comparison on this basis of the various arrangements.

It should be noted that all the hinge-moment results presented herein are for either 0.0057 or 0.0107 gap. Further tests appear desirable to obtain comparative results for arrangements with the gap sealed.

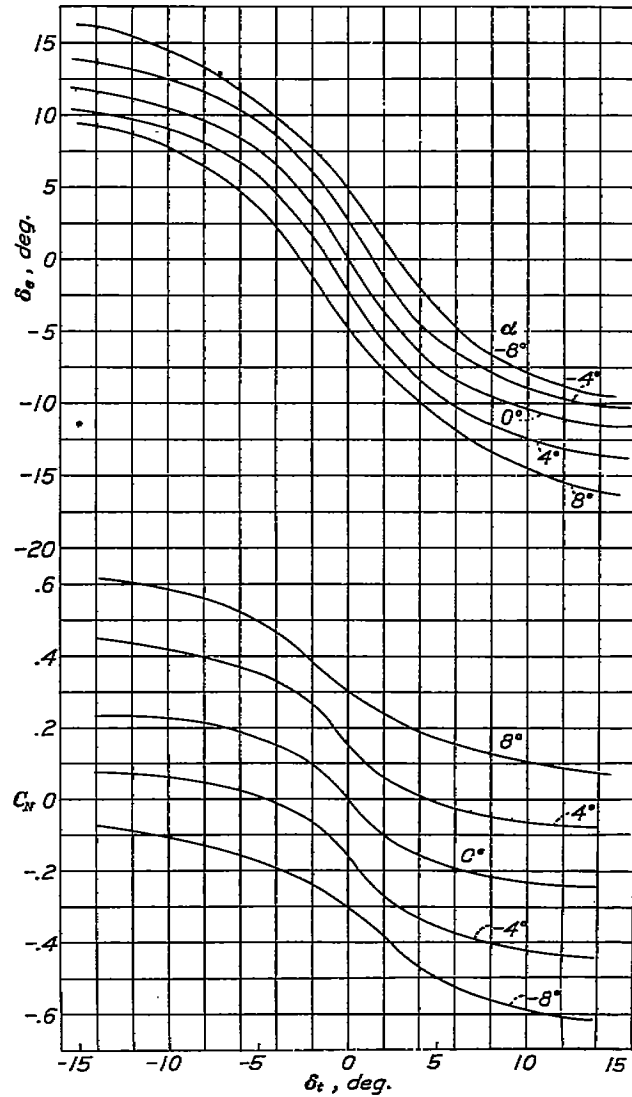


FIGURE 21.—Variation of  $\delta_e$  and  $C_N$  with  $\delta_t$ . Minimum-balance elevator.

TAB CHARACTERISTICS

The variation in elevator hinge-moment coefficient with angle of attack for various full-span tab and elevator deflections is shown in figure 16. These results are for minimum balance. There is a wide variation in tab effectiveness with  $\delta_e$ , the effectiveness being greatest at small elevator deflections. Figure 17, which is a cross plot of  $\Delta C_{h_e}$  against  $\delta_t$  (for  $\alpha=0^\circ$ ), shows that the tab effectiveness (for  $\delta_e=0^\circ$ ) decreases with  $\delta_t$  to about 50 percent of the computed value at  $\delta_t=-30^\circ$ . For elevator deflections of  $10^\circ$  and  $20^\circ$ ,

a larger variation from the computed values is observed and the effectiveness decreases still further at positive angles of attack. (See fig. 16.)

The relative effectiveness of partial-span tabs compared with full-span tabs is shown in figure 18. The change in hinge moment produced by a given tab

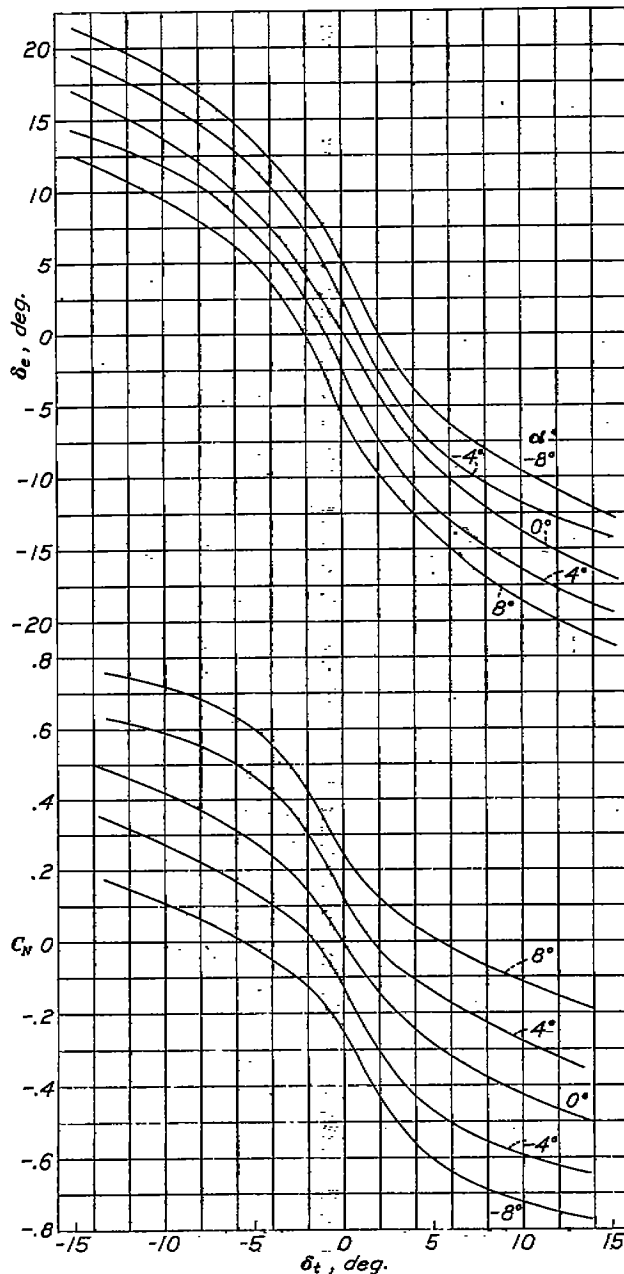


FIGURE 22.—Variation of  $\delta_e$  and  $C_N$  with  $\delta_t$ . 20-percent-balance; blunt-nose elevator.

deflection is approximately proportional to the area-moment of the tabs about the hinge line. Partial-span tab characteristics may thus be deduced by assuming the variation in  $\Delta C_{h_e}$  for a given tab deflection to be proportional to the ratio of the area-moment of the partial-span tab to that of the full-span tab. In this manner, partial-span tab characteristics similar to those given for the full-span tabs in figure 16 can be obtained.

Figure 19 shows the balancing effect of full-span, inboard and middle, and inboard tabs for various  $\delta_t/\delta_e$  ratios. If the tendency of tabs to overbalance at small elevator deflections is overcome (for example, by delaying the tab deflection until the elevator has been slightly deflected), the tab becomes a very effective balancing device. It also appears that still more desirable balancing characteristics can be obtained by the use of balance tabs in combination with a tapered-nose aerodynamic balance, which remains effective at large elevator deflections where the tab effectiveness falls off.

Figure 20 shows the variation of the stick-force criterion  $C_{h_e}\delta_e$  with  $C_N$  for various tab arrangements.

The rapid decrease in tab effectiveness at the larger tab and elevator deflections limits the use of tabs as a servocontrol device. This effect is shown in figure 21, which indicates the variation in elevator deflection  $\delta_e$  and normal-force coefficient  $C_N$  with tab deflection  $\delta_t$ . On an unbalanced elevator, the maximum change in  $\delta_e$  of  $\pm 12^\circ$  (measured from the free-floating position with  $\delta_t$  equal to  $0^\circ$ ) is obtainable with the full-span tab and corresponds to a  $\Delta C_N$  of  $\pm 0.30$ . These characteristics can be considerably improved, as shown in figure 22, if tabs are used on an elevator with aerodynamic balance. With the 20-percent blunt-nose balance, a  $\delta_e$  of about  $\pm 17^\circ$  and a  $\Delta C_N$  of  $\pm 0.50$  are obtained.

### CONCLUSIONS

1. The experimental variation of normal force with angle of attack ( $dC_N/d\alpha$ ) for the various tail arrangements was from 10 to 15 percent less than that computed from the aspect-ratio correction formula.
2. The presence of a gap caused a marked decrease in the value of the variation of normal force with elevator deflection ( $dC_N/d\delta_e$ ) but the size of the gap was unimportant (between 0.005 $\bar{c}$  and 0.010 $\bar{c}$ ) at angles below the stall. With some nose shapes, however, the larger gap caused an earlier stall.
3. The effect of aerodynamic balance varied greatly with nose shape. Tapered noses produced little balance at small elevator deflections but maintained the elevator effectiveness at much larger elevator deflections than did the blunt noses.
4. The decrease in normal force and hinge moment caused by the cut-out was proportional to the area removed.
5. The effectiveness of the tabs with change in span was approximately proportional to their area-moments about the elevator hinge line.

## APPENDIX

The computation of the characteristics of the tail surface, based on the thin-airfoil theory developed in reference 6, is used throughout the report as a basis for comparison. An outline of the computation follows.

The main characteristics of a flapped airfoil may be computed from the equations:

$$\begin{aligned} C_L &= a_1(\alpha + \lambda_1\delta_e + \lambda_2\delta_t) \\ C_{h_e} &= -u C_L - v_{11}\delta_e + v_{12}\delta_t \end{aligned}$$

where  $\lambda_1$ ,  $\lambda_2$ ,  $u$ ,  $v_{11}$ , and  $v_{12}$  are constants dependent upon the flap-chord ratios  $E_1$  and  $E_2$ ; their values have been determined by the thin-airfoil theory (reference 6). The lift-curve slope  $a_1$  is dependent upon aspect ratio and plan form.

The tail surface tested was designed so that the area ratios of the elevator and the tab corresponded approximately to their chord ratios over the span. The pertinent data and the necessary constants for the computation of the lift and the hinge-moment characteristics about the elevator hinge line are:

For elevator:

$$\frac{E_e}{E} = 0.41.$$

$$\lambda_1 = 0.753.$$

$$u = 0.121.$$

$$v_{11} = 0.0078.$$

For tab:

$$\frac{E_t}{E} = 0.08.$$

$$\lambda_2 = 0.357.$$

$$v_{12} = 0.0175.$$

The characteristics that can be determined (using the measured value of  $a_1 = 0.060$  except as noted) are:

$$\begin{aligned} \left(\frac{dC_L}{d\delta_e}\right)_\alpha &= \lambda_1 a_1 = 0.045 \\ &= 0.047 \text{ (for } a_1 = 0.063) \end{aligned} \quad (1)$$

The elevator-free lift-curve slope is obtained by setting  $C_{h_e} = 0$ . Then

$$\left(\frac{dC_L}{d\alpha}\right)_{C_{h_e}=0} = \frac{a_1}{1 + a_1\left(\frac{\lambda_1 u}{v_{11}}\right)} = 0.035 \quad (2)$$

$$\left(\frac{dC_{h_e}}{d\alpha}\right)_{\delta_e} = -u a_1 = -0.0073 \quad (3)$$

$$\left(\frac{dC_{h_e}}{d\delta_e}\right)_\alpha = -u \left(\frac{dC_L}{d\delta_e}\right)_\alpha - v_{11} = -0.0133 \quad (4)$$

$$\left(\frac{dC_{h_e}}{dC_L}\right)_\alpha = \frac{\left(\frac{dC_{h_e}}{d\delta_e}\right)_\alpha}{\left(\frac{dC_L}{d\delta_e}\right)_\alpha} = -0.295 \quad (5)$$

$$\left(\frac{dC_{h_e}}{d\delta_t}\right)_\alpha = -u \lambda_2 a_1 - v_{12} = -0.020 \quad (6)$$

The slope of the section lift curve for an N. A. C. A. 0009 section is 0.095, as determined from the data given in reference 4. By means of the aspect-ratio correction formula given in reference 7,

$$a_1 = f \frac{a_0}{1 + \frac{57.3 a_0}{\pi A}} \quad (7)$$

(where  $f=1$  for the plan form and the shape of the tail surface tested) a slope of 0.069 is determined for a tail surface of aspect ratio 4.7 and 2:1 taper.

### REFERENCES

1. Bradfield, F. B.: A Collection of Wind Tunnel Data on the Balancing of Controls. R. & M. No. 1420, British A. R. C., 1932.
2. Silverstein, Abe, and Katzoff, S.: Aerodynamic Characteristics of Horizontal Tail Surfaces. T. R. (to be published) N. A. C. A.
3. DeFrance, Smith J.: The N. A. C. A. Full-Scale Wind Tunnel. T. R. No. 459, N. A. C. A., 1933.
4. Goett, Harry J., and Bullivant, W. Kenneth: Tests of N. A. C. A. 0009, 0012, and 0018 Airfoils in the Full-Scale Tunnel. T. R. No. 647, N. A. C. A., 1938.
5. Harris, Thomas A.: Reduction of Hinge Moments of Airplane Control Surfaces by Tabs. T. R. No. 528, N. A. C. A., 1935.
6. Perring, W. G. A.: The Theoretical Relationships for an Aerofoil with a Multiply Hinged Flap System. R. & M. No. 1171, British A. R. C., 1928.
7. Anderson, Raymond F.: Determination of the Characteristics of Tapered Wings. T. R. No. 572, N. A. C. A., 1936.